

Patent 5,936,100 1999 (priority December 16, 1996); b) J. Louie, C. W. Bielawski, R. H. Grubbs, *J. Am. Chem. Soc.* **2001**, *123*, 11312–11313.

- [20] Insertion of Mg into commercial 6-bromo-1-hexene is accompanied by partial cyclization to give (cyclopentylmethyl)magnesium bromide in addition to the desired 5-hexenylmagnesium bromide, see D. Lal, D. Griller, S. Husband, K. U. Ingold, *J. Am. Chem. Soc.* **1974**, *96*, 6355–6357. The side products resulting thereof are easily eliminated by flash chromatography and the yield of **14** refers to analytically pure product.



Gaseous Gold Dihalides

Gold Dichloride and Gold Dibromide with Gold Atoms in Three Different Oxidation States**

Detlef Schröder,* Reuben Brown,
 Peter Schwerdtfeger, Xue-Bin Wang, Xin Yang,
 Lai-Sheng Wang, and Helmut Schwarz

Dedicated to Professor Roald Hoffmann
 on the occasion of his 65th birthday

While the most common oxidation states of gold are 0, I, and III, gold(II) compounds are also known to exist in the condensed phase and generally contain Au–Au bonds.^[1–2] However, genuine gold(II) chloride, AuCl₂, is not known in the condensed phase.^[3] Compounds such as CsAuCl₃ or

Au₄Cl₈ have been identified as mixed-valence species comprising Au^I and Au^{III} centers.^[4,5] Further, photooxidation of AuCl₂[–] ions in solution gives Au^{III} directly with no indication for the presence of Au^{II} intermediates,^[6] and the only report of Au^{II} in solution comes from a study by Rich and Taube in 1954 who proposed AuCl₃[–] as a transient in the redox reactions of Fe²⁺ and AuCl₄[–] ions.^[7]

Herein, we report an experimental and theoretical study of gaseous gold dihalides AuX₂^{–/0/+} (X = Cl, Br) bearing three different charges, that is, the AuX₂[–] ions (formally containing gold(I)), neutral AuX₂ species (formally gold(II)), and the corresponding AuX₂⁺ ions (formally gold(III)), provided that the latter species can still be described as ionized gold dihalides (see below).

To this end, two complementary experimental techniques are combined: photoelectron spectroscopy (PES)^[8] and sector-field mass spectrometry using charge-reversal (CR) and neutralization reionization (NR) techniques in conjunction with the related neutral-and-ion decomposition difference (NIDD) method.^[9,10] Both types of experiments start from the corresponding mass-selected AuX₂[–] ions as precursors. In the PES study, the AuX₂[–] ions (X = Cl, Br, I) are generated by electrospray ionization of diluted AuX solutions in water/methanol.^[11] In the sector experiments,^[12,13] fast-atom bombardment (FAB) of aqueous slurries of AuX₃ is used to generate AuX₂[–] ions; this method does not work for X = I, because reduction of AuI₃ to metallic gold occurs upon contact of the metallic probe tip with the sample. Likewise, no gold-fluoride ions could be generated by FAB of an AuF₃ slurry, because of the rapid hydrolysis of gold fluorides.

The photodetachment spectra of AuX₂[–] ions (X = Cl, Br, I) indicate substantial electron affinities for the corresponding neutral species (Figure 1). Thus, the vertical detachment energies amount to VDE(AuCl₂[–]) = 4.74 ± 0.05 eV, VDE(AuBr₂[–]) = 4.61 ± 0.05 eV, and VDE(AuI₂[–]) = 4.28 ± 0.05 eV. Adiabatic detachment energies, that is, the electron affinities (EAs) of the corresponding neutral species, can be estimated by linear extrapolation of the onsets of the first features to the baseline. This analysis leads to the values EA(AuCl₂) = 4.60 ± 0.07 eV, EA(AuBr₂) = 4.46 ± 0.07 eV, and EA(AuI₂) = 4.18 ± 0.07 eV. The relatively small differences (≤ 0.15 eV) between the vertical and adiabatic transitions indicate similar geometries for the anionic and neutral AuX₂^{–/0} species. Further, the PE spectra show several bands at higher energy which are assigned to the formation of electronically excited states in neutral AuX₂; these features will be analyzed in a forthcoming article. Here, we focus on the ground-state properties of the AuX₂^{–/0/+} systems and in particular for X = Cl.

Upon collisional activation of mass-selected AuCl₂[–] ions in the sector-field experiments, only the AuCl⁺ ion is detected as an anionic fragment. If the analyzer is switched to positive ions, the corresponding CR spectrum (Figure 2a) is dominated by the AuCl⁺ fragment (100%) along with a significant recovery signal for AuCl₂⁺ as well as the atomic Au⁺ ion; a weak signal from the Cl⁺ ion is detected at highest sensitivity (< 1%, not visible in Figure 2a). The NR spectrum of the AuCl₂[–] ion is also dominated by AuCl_n⁺ ions (n = 0–2), but the relative yield of AuCl⁺ is reduced significantly (Figure 2b).^[14]

[*] Dr. D. Schröder, Prof. Dr. H. Schwarz
 Institut für Chemie
 Technische Universität Berlin
 Strasse des 17. Juni 135, 10623 Berlin (Germany)
 Fax: (+49) 30-314-21102
 E-mail: df@www.chem.tu-berlin.de

Dr. R. Brown, Prof. Dr. P. Schwerdtfeger, Dr. X. B. Wang
 Department of Chemistry
 University of Auckland
 Private Bag 92019, Auckland (New Zealand)

Dr. X. Yang, Prof. Dr. L. S. Wang
 Department of Physics
 Washington State University
 2710 University Drive, Richland, WA 99352 (USA) and
 W. R. Wiley Environmental Molecular Science Laboratory
 Pacific Northwest National Laboratory
 P. O. Box 999, Richland, WA 99352 (USA)

[**] This work was supported by the Deutsche Forschungsgemeinschaft, the Fonds der Chemischen Industrie, the US National Science Foundation, and the Royal Society of New Zealand (Marsden scheme). The work in Washington was performed at the W. R. Wiley Environmental Molecular Science Laboratory, a national scientific user facility sponsored by Department of Energy's Office of Biological and Environmental Research which is operated for the US Department of Energy by Batelle. The Berlin group thanks the DEGUSSA AG for a gift of gold(III) halides. R.B. thanks the Alexander von Humboldt Stiftung (Bonn) for a research fellowship.

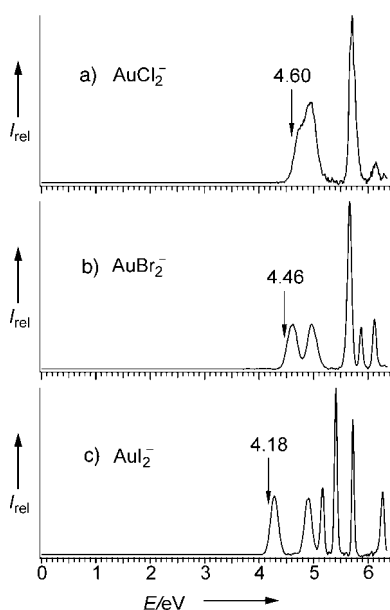


Figure 1. Photoelectron spectra of a) AuCl_2^- , b) AuBr_2^- , and c) AuI_2^- ions at 193 nm (6.424 eV). The derived adiabatic electron affinities of AuX_2 ($X = \text{Cl}, \text{Br}, \text{I}$) are indicated by the vertical arrows.

This qualitative difference between the CR and NR spectra indicates a notable difference between the more-or-less simultaneous detachment of two electrons in CR ($\text{AuCl}_2^- \rightarrow \text{AuCl}_2^+$) and the stepwise sequence of two single-electron detachments in NR (first $\text{AuCl}_2^- \rightarrow \text{AuCl}_2$, then $\text{AuCl}_2 \rightarrow \text{AuCl}_2^+$). The NIDD scheme^[10,15] allows for a quantification of the differential fragmentation behavior of AuCl_2^- upon CR and NR. In the NIDD spectrum of AuCl_2^- ions, the recovery signal and that of the Au^+ ions both appear on the positive scale, whereas the AuCl^+ fragment gives rise to a negative signal (Figure 2c).

These mass spectrometric results have the following implications. At first, the observation of an NR recovery signal demonstrates the existence of a transient neutral AuCl_2 species with a lifetime of at least several microseconds, that is, the time of flight between the two collision events. Next, the appearance of a recovery signal on the positive scale of the NIDD spectrum suggests that stepwise electron transfer in NR with intermediate relaxation of the neutral is associated with more favorable Franck–Condon factors than the direct CR of the anion. Likewise, the reversal of the $\text{AuCl}^+/\text{Au}^+$ ratios in CR and NR experiments suggests substantial differences of the potential-energy surfaces of anionic, neutral, and cationic $\text{AuCl}_2^{-/0/+}$ species. Furthermore, energy-resolved CR and NR measurements^[16] permit the determination of the energy balances of the associated redox transitions as $\Delta E_{\text{CR}} = 16.5 \pm 1.0$ eV and $\Delta E_{\text{NR}} = 16.0 \pm 1.0$ eV, respectively.^[17] To a first approximation, these energy differences correspond to those associated with the related vertical electron-transfer processes, that is, $\text{AuCl}_2^- \rightarrow \text{AuCl}_2^+$ in CR and first $\text{AuCl}_2^- \rightarrow \text{AuCl}_2$ then $\text{AuCl}_2 \rightarrow \text{AuCl}_2^+$ in NR.

For a more detailed analysis of the experimental results, the $\text{AuCl}_2^{-/0/+}$ system was studied theoretically using a scalar relativistic coupled-cluster approach (CCSD(T)).^[18–21] At this

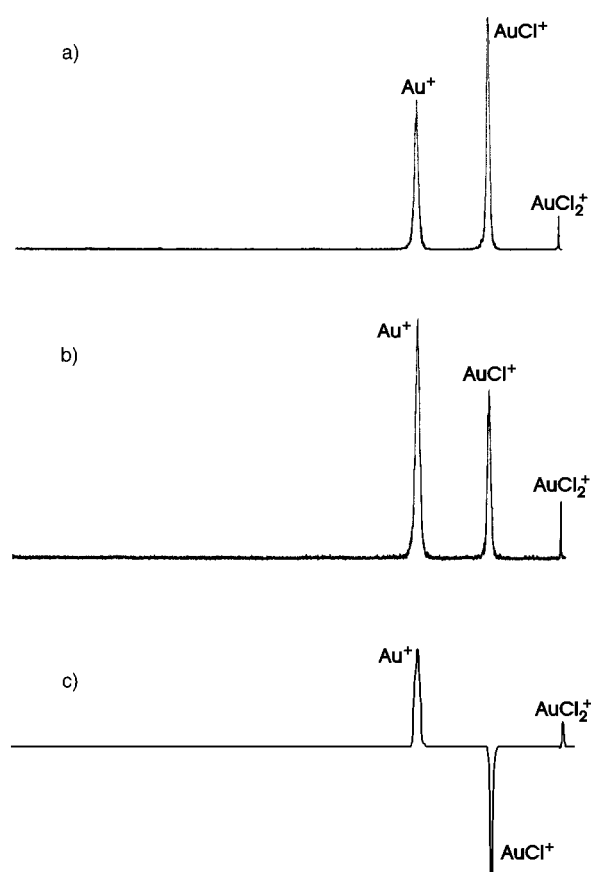


Figure 2. a) CR, b) NR, and c) NIDD mass spectra of mass-selected AuCl_2^- ions generated by FAB of an aqueous slurry of gold(III) chloride.

level of theory, the AuCl_2^- ion is predicted to have a singlet ground state ($^1\Sigma_g^+$) with a bond length of $r_{\text{AuCl}} = 2.29$ Å and an angle of $\alpha_{\text{ClAuCl}} = 180^\circ$ in good agreement with previous results.^[22] Likewise, a linear geometry is found for the neutral AuCl_2 species ($^2\Pi_g$, $r_{\text{AuCl}} = 2.25$ Å). The minor change in bond length ($\Delta r_{\text{AuCl}} = 0.04$ Å) is consistent with the similarity of the vertical and adiabatic detachment energies of AuCl_2^- ions in the PE spectra (see above). Note, however, that the Cl–Au–Cl bending potential is significantly softer for the neutral species than for the anion (Figure 3). Finally, the adiabatic and vertical detachment energies of the AuCl_2^- ion are

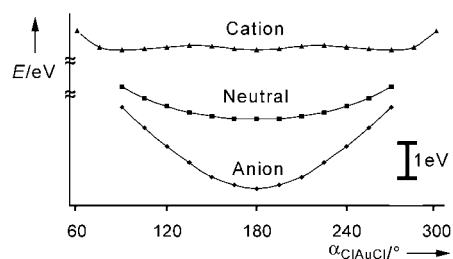


Figure 3. Schematic bending potentials of α_{ClAuCl} in AuCl_2^- , AuCl_2 , and AuCl_2^+ according to CCSD(T) calculations. To display the variations on a reasonable scale, the linear minima of the curves are deliberately fixed for a distance of 2 eV for each charge state.

calculated to be 4.77 and 4.85 eV, respectively, which is in good agreement with the experimental data.

A much more complicated situation evolves for the cationic species. For this triatomic AB_2 system, there are no less than three different low-lying minima on the singlet surface. A linear $AuCl_2^+$ ion ($^1\Pi_g$) with $r_{AuCl} = 2.21$ Å, a bent ($\alpha_{ClAuCl} = 94^\circ$), but otherwise similar $AuCl_2^+$ structure (1B_1 , C_{2v}) with $r_{AuCl} = 2.24$ Å, and a bent ion having a different connectivity of the atoms and C_s symmetry, that is, $Au(Cl_2)^+$ (1A_1) with $r_{AuCl} = 2.45$ Å, $r_{ClCl} = 2.06$ Å, and $\alpha_{ClAuCl} = 35^\circ$ (this corresponds to $\alpha_{AuClCl} = 102^\circ$). In terms of bonding schemes, the two former isomers can be viewed as gold dichlorides with a formal gold(III) center, whereas the third isomer is best described as an ion/neutral complex of atomic Au^+ and molecular chlorine.^[23] At the CCSD(T) level of theory, these three isomers are 0.72, 0.72, and 1.00 eV lower in energy than the corresponding dissociation asymptote $Au^+ + Cl_2$.^[24] The energetic proximity of the linear and bent $AuCl_2^+$ isomers has an analogy in the T-shaped structure of neutral $AuCl_3$ and the square-planar coordination in the corresponding dimer Au_2Cl_6 .^[25,26] Further, a bond strength of about 1 eV for the end-on complex of Au^+ with molecular chlorine is fully consistent with data for the ligation of gold(II) in the gas phase.^[27] For the linear isomer $AuCl_2^+$ ($^1\Pi_g$), the adiabatic and vertical ionization energies are computed as 10.71 and 10.79 eV, respectively (15.55 eV in total for the vertical transition $AuCl_2^- \rightarrow AuCl_2^+$).

The computed potential-energy surfaces of $AuCl_2^{-/0/+}$ (Figure 3 and 4) nicely account for the experimental findings. Thus, vertical charge reversal of the anion leads to the gold(III) dichloride cation $AuCl_2^+$ from which atomic chlorine is lost upon consecutive fragmentation in the high-energy collision event. In contrast, neutralization of the anion provides access to the neutral species having a much flatter Cl-Au-Cl bending potential. Upon reionization of neutral $AuCl_2$, the bent $AuCl_2^+$ ion and in particular the more stable $Au(Cl_2)^+$ isomer can be formed, thereby accounting for the positive NIDD signal of the recovery ion. In addition, the structural reorganization associated with bending increases the probability of access to the low-lying $Au^+ + Cl_2$ dissoci-

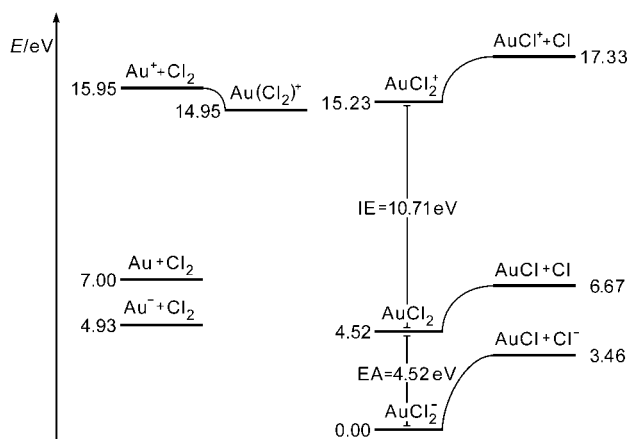


Figure 4. Redox profile of $AuCl_2^-$, $AuCl_2$, and $AuCl_2^+$ according to CCSD(T) calculations (energies [eV] relative to the anion). For the sake of clarity, the bent minimum of $AuCl_2^+$ is omitted (see text).

ation asymptote in the NR experiment, thereby accounting for the positive NIDD signal for the Au^+ fragment. It is instructive to consider the computed Au-Cl dissociation energies (D_0) of the linear $AuCl_2^{-/0/+}$ species as a function of charge. The calculated values are, $D_0(ClAu-Cl^-) = 3.45$ eV for the anion, $D_0(ClAu-Cl) = 2.15$ eV for the neutral, and $D_0(ClAu^+-Cl) = 2.10$ eV for the cation indicate that all three species can be termed as being covalently bound metal halides. Accordingly, gaseous gold dichloride can exist in three different oxidation states.^[23]

A comparable situation seems to occur in the $AuBr_2^{-/0/+}$ system. Thus, the PE detachment energies are similar to those of the dichloride, and the $AuBr_n^+$ fragments ($n=0-2$) detected by CR and NR of mass-selected $AuBr_2^-$ ions (intensities in CR/NR, respectively: $AuBr_2^+$: 25/55, $AuBr^+$: 100/100, Au^+ : 25/45) lead to positive NIDD signals for the $AuBr_2^+$ recovery ion as well as atomic Au^+ ion, whereas that of the $AuBr^+$ ion is negative. Preliminary theoretical calculations of the linear $AuBr_2^{-/0/+}$ isomers indicate a situation quite similar to that of $AuCl_2^{-/0/+}$.

In summary, mass spectrometric experiments demonstrate that the gold dihalides AuX_2 ($X=Cl, Br$) can adopt three different oxidation states, all giving rise to long-lived triatomic species in the gas phase. As far as the stability of gold(II) halides in the condensed phase is concerned, the combination of the calculated enthalpy of bonding $\Delta_f H(AuCl_2) = 30$ kcal mol⁻¹^[28] as predicted by theory with $\Delta_f H(AuCl) = 50$ kcal mol⁻¹^[30] and $\Delta_f H(AuCl_3) = 48$ kcal mol⁻¹^[31] suggests that disproportionation of neutral gold(II) dichloride according to reaction in Equation (1) is endothermic by 38 kcal mol⁻¹.^[32]



Thus, whereas $AuCl_2$ is stable against disproportionation in the idealized gas phase, it is likely to exist as $Au^+[AuCl_4]^-$ in the condensed phase. The preparation of bulk gold(II) compounds therefore requires an appropriate ligand environment to prevent disproportionation. An excellent example for such a stabilization of a gold(II) compound by ligation is the $AuXe_4^{2+}(Sb_2F_{11})_2^-$ salt recently characterized by Seidel and Seppelt.^[33,34]

Received: October 21, 2002 [Z50405]

- [1] R. J. Puddephatt, *The Chemistry of Gold*, Elsevier, Amsterdam, 1978.
- [2] See also: W. Grochala, R. Hoffmann, *Angew. Chem.* **2001**, *113*, 2817; *Angew. Chem. Int. Ed.* **2001**, *40*, 2742.
- [3] *Gmelin Handbook of Inorganic and Organometallic Chemistry*, Au, Suppl. B1, **1992**, p. 189.
- [4] N. Elliot, L. Pauling, *J. Am. Chem. Soc.* **1938**, *60*, 1846.
- [5] D. Belli Dell'Amico, F. Calderazzo, F. Marchetti, S. Merlini, G. Perego, *J. Chem. Soc. Chem. Commun.* **1977**, 31, and references therein.
- [6] H. Kunkely, A. Vogler, *Inorg. Chem.* **1992**, *31*, 4539.
- [7] R. L. Rich, H. Taube, *J. Phys. Chem.* **1954**, *58*, 6.
- [8] L. S. Wang, C. F. Ding, X. B. Wang, S. E. Barlow, *Rev. Sci. Instrum.* **1999**, *70*, 1957.
- [9] N. Goldberg, H. Schwarz, *Acc. Chem. Res.* **1994**, *27*, 347.

- [10] a) C. A. Schalley, G. Hornung, D. Schröder, H. Schwarz, *Chem. Soc. Rev.* **1998**, 27, 91; b) C. A. Schalley, G. Hornung, D. Schröder, H. Schwarz, *Int. J. Mass Spectrom. Ion Processes* **1998**, 172, 181.
- [11] The PES apparatus includes a magnetic-bottle time-of-flight photoelectron analyzer and an electrospray ion source as described elsewhere.^[8] In brief, 10^{-3} molar solutions of AuX in water/methanol (1/9; pH ~ 7) were sprayed through a 0.01 mm diameter syringe needle at ambient atmosphere and a potential of -2.2 kV. Negatively charged ions emerging from the source were guided by an rf-only quadrupole into an ion trap, where the ions were accumulated for 0.1 s before being pushed into the extraction zone of a time-of-flight mass spectrometer. The major anions were AuX_2^- and AuX_4^- . In the PES experiments, the anions of interest were mass-selected, decelerated, and intercepted by a 193 nm laser beam in the detachment zone of the magnetic-bottle photoelectron analyzer. The photoelectrons were collected near 100% efficiency and analyzed in a four-meter long time-of-flight tube. Photoelectron time-of-flight spectra were then converted into kinetic energy spectra and calibrated against the known spectra of O^- and I^- ions.
- [12] The experiments were performed with a modified VG ZAB/HF/AMD 604 four-sector mass spectrometer of BEBE configuration (B stands for magnetic and E for electric sectors).^[13] The ions of interest were generated by FAB (Xe, 8–10 kV) of aqueous slurries of AuX_3 in the negative-ion mode. The ions having a kinetic energy of 8 keV were mass-selected using B(1) and the respective mass spectra were recorded by scanning E(1). For collisional activation, helium was used as the collision gas at 80% transmission (T). In the CR and NR experiments,^[9,10] oxygen was used throughout as the collision gas (80% T).
- [13] C. A. Schalley, D. Schröder, H. Schwarz, *Int. J. Mass Spectrom. Ion Processes* **1996**, 153, 173.
- [14] The absolute ratio of the survivor signals in CR and NR is approximately 4:1.
- [15] The NIDD intensities are derived from the NR and CR spectra using the following formula: $I_{i,\text{NIDD}} = I_{i,\text{NR}}/\Sigma I_{i,\text{NR}} - I_{i,\text{CR}}/\Sigma I_{i,\text{CR}}$; for further details, see ref. [10b].
- [16] a) D. Schröder, S. Bärsch, H. Schwarz, *Int. J. Mass Spectrom.* **1999**, 192, 125; b) D. Schröder, H. Schwarz, *Int. J. Mass Spectrom.*, in press.
- [17] Note that the majority of the experimental error arises from uncertainties in the calibration of the kinetic energy scale.^[16] The experimental difference of ΔE_{CR} and ΔE_{NR} is 0.5 ± 0.3 eV.
- [18] The calculations were performed using the Gaussian98 program^[19] at the CCSD(T) level. For gold, an adjusted valence basis set together with a small-core scalar relativistic pseudopotential was used which consists of a $[\text{Kr}]4d^{10}4f^{14}$ core ($5s^25p^65d^{10}6s^1$ valence space).^[20] For the halogen atoms, augmented, correlation-consistent, double- ζ basis sets were employed. Some initial CCSD(T) geometry optimizations were performed with single- ζ basis sets and were then repeated with the larger aug-cc-pVDZ basis set; at this level only partial re-optimization of the geometries was performed.
- [19] Gaussian98 (Revision A.7), M. J. Frisch, G. W. Trucks, H. B. Schlegel, G. E. Scuseria, M. A. Robb, J. R. Cheeseman, V. G. Zakrzewski, J. A. Montgomery, R. E. Stratmann, J. C. Burant, S. Dapprich, J. M. Millam, A. D. Daniels, K. N. Kudin, M. C. Strain, O. Farkas, J. Tomasi, V. Barone, M. Cossi, R. Cammi, B. Mennucci, C. Pomelli, C. Adamo, S. Clifford, J. Ochterski, G. A. Petersson, P. Y. Ayala, Q. Cui, K. Morokuma, D. K. Malick, A. D. Rabuck, K. Raghavachari, J. B. Foresman, J. Cioslowski, J. V. Ortiz, B. B. Stefanov, G. Liu, A. Liashenko, P. Piskorz, I. Komaromi, R. Gomperts, R. L. Martin, D. J. Fox, T. Keith, M. A. Al-Laham, C. Y. Peng, A. Nanayakkara, C. Gonzalez, M. Challacombe, P. M. W. Gill, B. G. Johnson, W. Chen, M. W. Wong, J. L. Andres, M. Head-Gordon, E. S. Replogle, J. A. Pople, Gaussian, Inc., Pittsburgh, PA, **1998**.
- [20] P. Schwerdtfeger, M. Dolg, W. H. E. Schwarz, G. A. Bowmaker, P. D. W. Boyd, *J. Chem. Phys.* **1989**, 91, 1762.
- [21] For a similar approach, see: J. R. Brown, P. Schwerdtfeger, D. Schröder, H. Schwarz, *J. Am. Soc. Mass Spectrom.* **2002**, 13, 485.
- [22] P. Schwerdtfeger, P. D. W. Boyd, A. K. Burrell, W. T. Robinson, M. J. Taylor, *Inorg. Chem.* **1990**, 29, 3593.
- [23] These bonding schemes are fully consistent with Mulliken population analysis of the partial charges: AuCl_2^- , $q_{\text{Au}} = 0.44$, $q_{\text{Cl}} = -0.72$; AuCl_2^0 , $q_{\text{Au}} = 0.80$, $q_{\text{Cl}} = -0.40$; AuCl_2^+ (${}^1\Pi_g$), $q_{\text{Au}} = 1.02$, $q_{\text{Cl}} = -0.01$; AuCl_2^+ (1B_1), $q_{\text{Au}} = 1.09$, $q_{\text{Cl}} = -0.045$; $\text{Au}(\text{Cl}_2)^+$ (1A_1), $q_{\text{Au}} = 0.85$, $q_{\text{Cl}(1)} = -0.01$, $q_{\text{Cl}(2)} = 0.16$.
- [24] We note that the relative energies of the three cationic isomers, differed significantly between single- and double- ζ basis sets. As also the double- ζ basis is far from being complete and spin-orbit effects are neglected, the energy order of the $[\text{AuCl}_2]^+$ isomers should accordingly be viewed as a first approximation.
- [25] P. Schwerdtfeger, P. D. W. Boyd, S. Brienne, A. K. Burrell, *Inorg. Chem.* **1992**, 31, 3411.
- [26] M. Hargittai, A. Schulz, B. Reffy, M. Kolonits, *J. Am. Chem. Soc.* **2001**, 123, 1449.
- [27] D. Schröder, H. Schwarz, J. Hrušák, P. Pyykkö, *Inorg. Chem.* **1998**, 37, 624.
- [28] Calculated for 0 K using the enthalpy of the reaction $\text{AuCl}_2 \rightarrow \text{Au} + \text{Cl}_2$ computed here as $57.3 \text{ kcal mol}^{-1}$ in conjunction with $\Delta_f H(\text{Au}) = 87.5 \text{ kcal mol}^{-1}$ and $\Delta_f H(\text{Cl}_2) = 0 \text{ kcal mol}^{-1}$ taken from ref. [29].
- [29] S. G. Lias, J. E. Bartmess, J. F. Liebman, J. L. Holmes, R. D. Levin, W. G. Mallard, *J. Phys. Chem. Ref. Data Suppl. 1* **1988**, 17.
- [30] Calculated for 0 K using the values $\Delta_f H(\text{Au}) = 87.5 \text{ kcal mol}^{-1}$, $\Delta_f H(\text{Cl}) = 28.6 \text{ kcal mol}^{-1}$, and $D_0(\text{Au}-\text{Cl}) = 66 \text{ kcal mol}^{-1}$ taken from refs. [21] and [29].
- [31] Calculated for 0 K using $\Delta_f H(\text{Au}_2\text{Cl}_6) = 47 \text{ kcal mol}^{-1}$ and the computational prediction of $D_0(\text{Cl}_3\text{Au}-\text{AuCl}_3) = 48.4 \text{ kcal mol}^{-1}$ taken from: a) D. D. Wagman, W. H. Evans, V. B. Parker, R. H. Schumm, I. Halow, S. M. Bailey, K. L. Churney, R. L. Nuttal, *J. Phys. Chem. Ref. Data Suppl. 1* **1982**, 11; b) ref. [25].
- [32] The directly calculated B3LYP value is 24 kcal mol^{-1} , see: R. Brown, Ph.D. Thesis, University of Auckland, New Zealand, **2001**.
- [33] S. Seidel, K. Seppelt, *Science* **2000**, 290, 117.
- [34] See also: T. Drews, S. Seidel, K. Seppelt, *Angew. Chem.* **2002**, 114, 470; *Angew. Chem. Int. Ed.* **2002**, 41, 454.